75th International Astronautical Congress (IAC), Milan, Italy, 14-18 October 2024.

IAC-24-A6.10-E9.4.4

LOW EARTH ORBIT CAPACITY THRESHOLDS INVESTIGATION FOR A SUSTAINABLE USE OF THE SPACE ENVIRONMENT

Andrea Muciaccia [a,*], **Francesca Letizia**[b], **Mirko Trisolini** [c], **Giudici Lorenzo** [a], **Stijn Lemmens** [b], **Juan Luis Gonzalo** [a], **Camilla Colombo** [a],

[a] *Department of Aerospace Science and Technology, Politecnico di Milano, Via La Masa 34, 20156, Milan, Italy. andrea.muciaccia@polimi.it, lorenzo.giudici@polimi.it, juanluis.gonzalo@polimi.it, camilla.colombo@polimi.it*
[b] *ESA/ESTEC, Independent Safety Office, Keplerlaan 1, 2201 Noordwijk, The Netherlands. francesca.letizia@esa.int, francesca.letizia@esa.int*
[c] *Vyoma GmbH, Karl-Theodor-Straße 55, 80803 München, Germany. mirko.trisolini@vyoma.space*
[*]Corresponding author: andrea.muciaccia@polimi.it

Abstract

The increase in the number of orbiting objects, being them controllable or uncontrollable, is expected to significantly affect space operations in the near future. This is particularly true in the Low Earth Orbit (LEO) region, where the population of debris is increasing because of new fragmentation, while, at the same time, the advent of large constellations has accelerated the growth of the number of active missions. Therefore, careful mission design together with the implementation of mitigation guidelines and policies are essential to regulate the evolution of space environment and to avoid the proliferation of derelict objects around the Earth. In this view, in recent years, international discussion is ongoing on how to assess space capacity and how this concept could be improved and exploited to define actionable thresholds to be used to define specific mission requirements.

This work aims at analysing the threshold of orbital capacity, investigating the evolution of the space environment with long-term simulation scenarios defined in terms of launch traffic, explosions rate, and disposal strategies. In this context, a risk metric, considering the likelihood and associated severity of fragmentation of the satellite(s), is used to measure the impact of each mission on the environment and subsequent space capacity consumption. The metric is applied to each mission and in each scenario, both at the beginning and at the end of the simulation, to evaluate the change in total capacity consumption. The latter is further investigated in terms of type of in-orbit objects analysed (e.g., payloads, constellations), orbital areas in which they are located (e.g., altitude slots), and eventual designated post-mission disposal strategy, along with its reliability. Several scenarios, based on historical trends or on extrapolation of current behaviours, are considered, subjected to Monte Carlo simulation, and compared to understand the relevance of each parameter and their adherence to a sustainable evolution of space.
Keywords: Space Debris, Space Capacity, Space Sustainability, Space Traffic Management

Nomenclature

a [km]	Semi-major axis
C [-]	Capacity value
e_c [-]	Severity of a collision fragmentation event
e_c [-]	Severity of an explosion fragmentation event
I [-]	Space debris index at a single epoch
I_t [-]	Total space debris index of a mission
p_c [-]	Probability of collision
p_e [-]	Probability of explosion

Acronym/Abbreviations

DISCOS	Database and Information System Characterising Objects in Space
ECOB	Environmental Consequences of Orbital Breakups
EOL	End-Of-Life
ESA	European Space Agency
GEO	Geosynchronous Earth Orbit
GTO	Geostationary Transfer Orbit
LEO	Low Earth Orbit
MC	Monte Carlo
MEO	Medium Earth Orbit
PIB	Particle-In-a-Box
PMD	Post Mission Disposal
THEMIS	Tracking the Health of the Environment and Missions In Space

1. Introduction

The sustainability of the space around the Earth is becoming an increasingly important issue in the space sector. The occurrence of breakup events that increase the background population of inactive objects and the increase of large constellations that place many satellites in specific orbital regions (particularly in LEO) [1], led to the improvement and definition of new mitigation policies and careful mission design (with particular attention to End-Of-Life (EOL) strategies). Parallel to this, several risk metrics [2] [3] have been developed in the past years to assess the impact of missions on the space environment (each of which seeks to capture the main elements that influence it) and the status of the space environment itself (with a focus on the debris population). These metrics could be a useful tool to further improve the mitigation guidelines.

More recently, the study of space sustainability has also begun to focus on the problem of the capacity of the space environment. In fact, space, like other ecosystems, is a finite resource, which must therefore be managed in such a way to have it available also in the future. Current models base their formulations either on the risk metrics (e.g., Letizia et al.[4]) or on the investigation of the number of active satellites that can be launched and kept in orbit [5], and are usually linked to environment models whose aim is to predict the long-term evolution of the debris population. Most of them fall into the category of semi-deterministic approaches (piece wise propagation of the population of orbiting objects, examples are [6] [7] [8] [9]), while others are referred to as Particle-In-a-Box (PIB) models (source-sink models describing the evolution of different species of objects) [10] [11] [12].

In this work, the concept of orbital capacity is exploited to study the level of risk of a fragmentation on the space environment [13]. Indeed, the aim of the work is to understand if the capacity concept can be used to properly assess the severity of a fragmentation and rank it according to some specific parameters. Each fragmentation is characterised by several parameters, which influence what the severity of the fragmentation may be on the population of orbiting objects. Thus it is essential to understand its impact both from a short- and a long-term point of view.

The paper is organised as following: Section 2 briefly describes the main feature of the metric adopted for the study. Section 3 introduces the model with which the risk level of a fragmentation is investigated, while Section 4.1 shows the results of the tests performed on fictitious fragmentation. A conclusive section summarises the main achievement and future works.

2. Space capacity evaluation

2.1 Space debris index definition

The assessment of space capacity, as modeled in this work, is based on a metric defined to assess the impact of missions on the space environment. The THEMIS space debris index [14] [15] is defined as a risk indicator and follows the formulation of the Environmental Consequences of Orbital Breakups (ECOB) index [16]. The developed index can be used for different mission architectures (e.g., single satellite, constellation, etc.) [17] [18] and in different orbital regions, such as Low Earth Orbit (LEO), Medium Earth Orbit (MEO), Geostationary Transfer Orbit (GTO), Geosynchronous Earth Orbit (GEO) [15] [19].

Focusing on the LEO orbital region, the model considers the orbit semi-major axis and inclination of the investigated object as study parameters [13] [15], being them the main mission parameters when considering objects in LEO orbit.

The evaluation is performed along the entire lifetime of the mission (accounting for each possible phase of the mission) by computing the total debris index of a mission I_t as

$$I_t = \int_{t_0}^{t_{EOL}} I(t)\,dt + \alpha \int_{t_{EOL}}^{t_{end}} I(t)\,dt + (1-\alpha) \int_{t_{EOL}}^{t_f} I(t)\,dt \tag{1}$$

where the first term of Eq. 1 refers to the operational phase of the object, while the second and the third term to the Post Mission Disposal (PMD) phase where the failure of the End-Of-Life (EOL) disposal is considered. The latter is taken into account through the PMD reliability α ranging between 0 (fail) and 1 (fully reliable). In the formulation, $I(t)$ stands for the debris index at a single epoch

$$I = p_c \cdot e_c + p_e \cdot e_e \tag{2}$$

with p_c and p_e the probability of collision and explosion, and e_c and e_e the severity of a collision or of an explosion (i.e., the effects of the breakup in given orbital region), respectively. Being outside the scope of this paper, a more in-depth description of the different terms can be found in [14] [20] [21] or in Appendix A. Although not directly explicit, the formulation internally considers many factors such as: the mass and the cross-sectional area of the object, the Collision Avoidance Manoeuvres (CAM) capabilities (and their efficacy), the type of PMD (e.g., re-entry, graveyard). All these parameters play a role in the computation of the index, increasing or decreasing the impact of the mission on the space environment.

2.2 Space capacity definition

Starting from the definition of the space debris index, the space capacity consumed by a defined population of orbiting objects is computed by aggregating the debris index value of each single mission as [15]

$$C = \sum_{j=1}^{N_{missions}} I_{t_j} \tag{3}$$

where I_{t_j} is the index of the $j-th$ object considered in the set, and $N_{missions}$ is the total number of objects (either active or inactive) considered in the analysis. Thus, the index can be currently seen as the share of the capacity of the specific mission under analysis.

3. Impact of fragmentation on space environment using the capacity concept

3.1 Fragmentation events risk level

Since 1957, the number of artificial space objects has grown constantly [1], undergoing an increase in the recent years due to the introduction of several satellite-based services. This, however, has also led to an increase in the collision or explosion events, involving the generation of new debris. Indeed, despite the presence of guidelines for the space debris mitigation and collision avoidance, some events are difficult to predict (e.g., collision between objects) or even unpredictable (e.g., explosion of a rocket body). The growth of the space debris population is a serious concern since it poses space regions under higher risks, that can even lead to fragmentation chain effects [22]. Tools have been developed to detect those fragmentations, characterise them and investigate the risk caused by the generated fragments on the population of orbiting objects, with an eye toward the active satellites.
However, it is also important to understand and quantify the impact, and hence the level of risk, posed by a new fragmentation event over short- and long- period of time. The impact should be considered not only in terms of the number of objects added to the environment, but also for how long they will be there and how they interact with the already orbiting objects. In this view, the concept of the capacity tries to consider the problem from different perspective.
In order to quantify the risk level of a fragmentation, one must start from the consideration that each fragmentation event is characterised by different parameters, such as

- Type of event (e.g., collision, explosion) and number of objects involved: each type of fragmentation is characterised by a different energy level, that thus is linked to a different number of fragments generated (as it is modeled in the NASA Standard Breakup Model [23]). An example is shown in Figure 1, with a comparison between the evolution over time of the number of objects generated by an explosion and a catastrophic collision fragmentations. For this example, the fragmentation was simulated in the same location and considering the same total mass.
- Location of the event (e.g., altitude, inclination) and geometry of the orbit(s): this influences on the one hand the possible interaction with crowded regions that will have to interact with the generated fragments, but also the types of orbital perturbations influencing the short- and long- term evolution of the fragments. Indeed, as can be seen from Figure 2, two breakup events (of the same type) were simulated at different altitudes and the one at lower altitude (green line) is characterised by a faster reduction of the number of objects (larger than 1 cm in the figure) in orbit over time thanks to the effect of the atmospheric drag. The results are normalised with respect to the number of fragments generated.

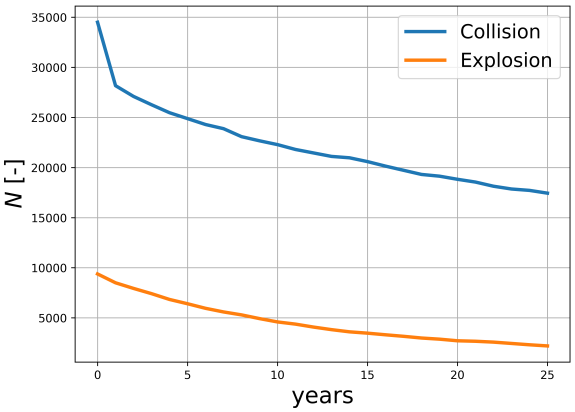

Fig. 1. Comparison in terms of evolution over time of the number of fragments generated by a collision event (in blue) and an explosion event (in orange).

3.2 Model workflow

The model is based on the comparison of two scenarios: the first in which the evolution over time (using an environmental evolutionary model) of a population (referred to as the reference population) of objects is assessed, and the second in which the same evolution is investigated but a fragmentation is added to the reference population. Then, a metric is introduced to investigate the difference between the two evolutionary trends.
The scenario is defined in terms of initial population (of orbiting objects), launch traffic and PMD strategy, while each fragmentation event can be characterised in terms of type of event (e.g., collision or explosion), mass involved, and location (here in terms of orbit altitude and inclination).
The results of the environmental evolutionary model includes the number of objects (at different snapshot epochs),

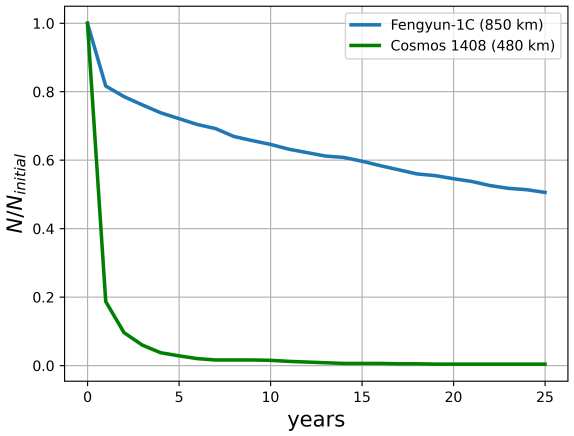

Fig. 2. Comparison in terms of evolution over time of the number of fragments generated at higher altitude (in blue) and at lower altitude (in green). The results are normalised with respect to the number of fragments generated at time 0.

their characteristics (e.g., Keplerian orbital elements and physical properties of each single object), and the number of events that occurred during the period considered. In addition to these results, the capacity consumed by the population can be computed at different snapshot epochs to see its evolution over time and to use it to compare the two scenarios.

The evaluation of the evolution of both the reference scenario and of the scenario including the fragmentation event is simulated several times using a Monte Carlo (MC) approach to increase the statistical relevance of the investigation. This implies that several evolution of the same scenario are available, generating a distribution of data for the different results (including the capacity evaluated at different snapshot epochs).

The comparison of the two scenarios is hence performed comparing the distribution in terms of consumed capacity (i.e., the aggregated values of the impact of each single mission, here computed using THEMIS software) of the two cases to understand if and how much the two behaviours differ from each other. To do so, the one-tailed Z-test (typically used to compare two normal distributions) is used considering the following null and alternative hypotheses

$$\begin{cases} H_0 : C_{frag} = C_{ref} \\ H_0 : C_{frag} > C_{ref} \end{cases} \tag{4}$$

with C_{frag} describing the distribution of the capacity when including the fragmentation, while C_{ref} is the distribution of the reference scenario. The alternative hypothesis is defined considering only the $>$ because the investigation is performed to understand if (and how much) the capacity level is higher when adding the fragmentation event.

The Z-score (that is the metric of the test) is computed at each epoch (y) as follow

$$Z_y = \frac{\bar{C}_{frag_y} - \bar{C}_{ref_y}}{\sqrt{\sigma^2_{C_{frag_y}} + \sigma^2_{C_{ref_y}}}} \tag{5}$$

where $\bar{C}_{frag_y}$ is the mean value of the fragmentation scenario at the $y-th$ epoch, $\bar{C}_{ref_y}$ is the mean value of the reference scenario at the $y-th$ epoch, and $\sigma^2_{C_{frag_y}}$ and $\sigma^2_{C_{ref_y}}$ are the standard deviation divided by the square root of the number of MC considered.

Then, according to statistics, three risk levels are currently defined as shown in Figure 3. Whenever the Z score is above 3.1, the evolution of the environment is considered to be highly different from the reference scenario, while below 1.96 the two behaviours can be considered as similar.

The score can be used in two different ways: to assign a risk level to a fragmentation event and to investigate its evolution over time to see if and when the evolution would fall within the reference scenario.

Figure 4 shows a block-diagram of the model.

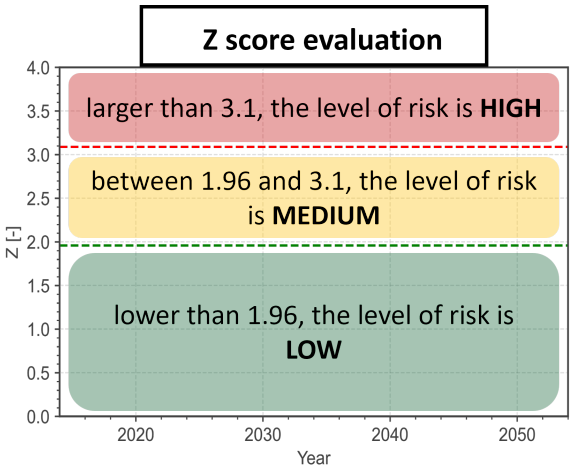

Fig. 3. Classification of risk level according to the Z-score.

Similar approaches can be found in the literature, where past works have already tried to analyse the problem, leading to the development of analytical indexes to rank the fragmentation events and the severity of the fragmentation of the objects on the environment [24] [25].

3.3 Reference scenario

The reference scenario used in this work considers the population of orbiting objects in orbit as of 1^{st} January 2014 [4] (as available in ESA DISCOS), considering the following properties for the long-term evolution of the space environment:

- Launch traffic repeated every 5 years, considering historical data from 2009 to 2014 available in

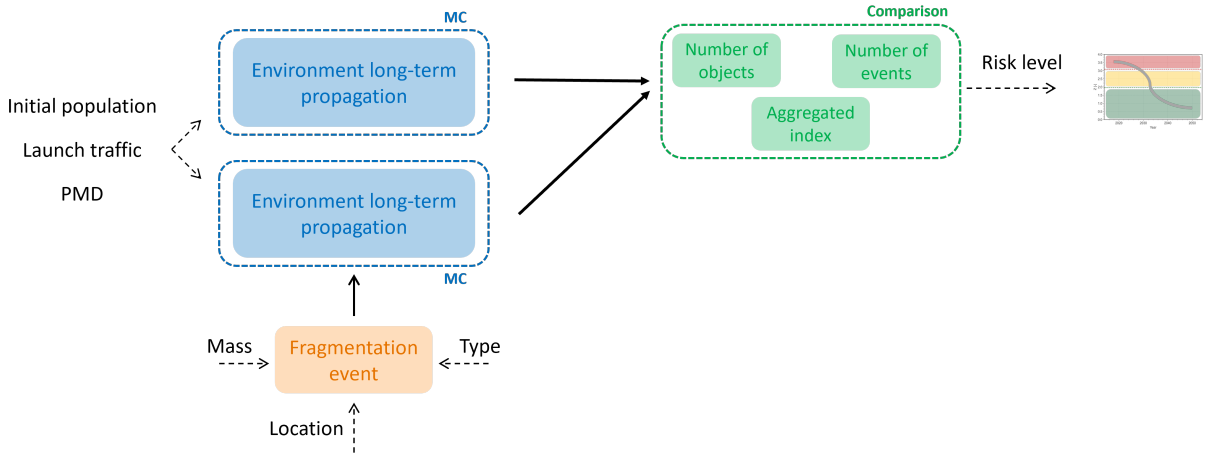

Fig. 4. Risk level evaluation - model workflow.

ESA DISCOS database (including data not publicly available) [ref].

- Lifetime for each single object of 8 years.
- Fragmentation event due to explosion discarded (assumption considered also in past works [24]). This hypothesis is introduced in order to investigate the impact of collision events, only.
- Collision avoidance capabilities disabled (assumption considered also in past works [24]).
- Constellations discarded (still considering any objects already launched).

The reference scenario was propagated 200 years using the ESA DELTA4 [6] evolutionary model into the future by running 40 MC simulations (computational limits of internal server facility). Figure 5 shows the evolution in the number of objects lager than 10 cm over time, where the dark line represents the average value while the light lines the lower and upper limits obtained from the simulations.. As expected, the number is increasing because of fragmentation events.

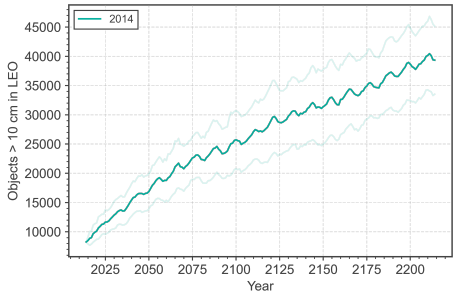

Fig. 5. Evolution over time of the number of objects larger than 10 cm in LEO.

4. Fragmentation events investigation

This section is dedicated to the description of the test cases performed with the developed model. The tests involved fragmentations generated at different locations and with different masses.
Looking at the results obtained and past work [24], it was decided to focus in the evaluation of capacity in the first years after fragmentation (while still having results available for the final part as well). behavior is usually much more distant from the baseline scenario than what happens away from the fragmentation.

4.1 Fragmentation location

For the tests described in this work, the locations of the investigated fragmentation was not randomly selected, but the severity maps (used in the index formulation, see Appendix A) were used as a starting point. Indeed, from those maps it is possible to understand which regions would affect more the population of active objects in case of fragmentation (mainly from a cumulative collision point of view).
For the purpose of this work, three location have been considered in terms of orbit altitude and inclination. The study parameters are included in Table 1, and the location of the fragmentation is displayed in Figure 6. The three location were selected to include the peak of the map (that is the location that will mostly affect the population in case of a fragmentation), the location of the active satellites, and an higher altitude object. In addition, only catastrophic collisions were considered.

Table 1. Characteristics of the fragmentation event.

Altitude [km]	800, 1600
Inclination [deg]	80, 100
Mass [kg]	500, 1000, 4000, 8000

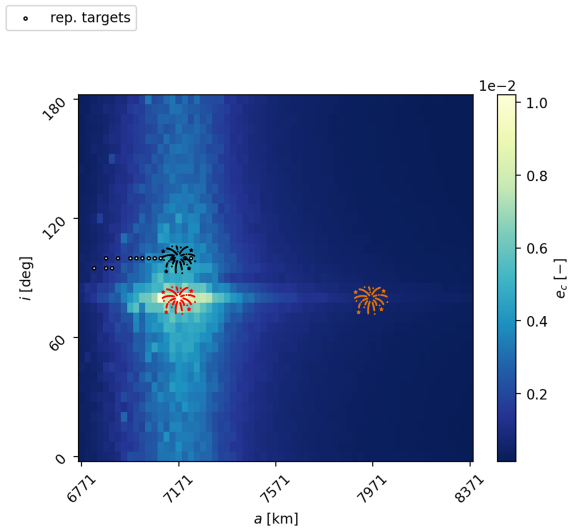

Fig. 6. Catastrophic collision effect maps computed considering targets at 01-01-2014 with the location of the fragmentation on top.

4.2 Space capacity Z-score evolution for fragmentation in different location

As said in the previous section, three different location (in terms of orbit altitude and inclination) where considered for the fragmentation.

A fragmentation involving a mass of 4000 kg was simulated at an altitude of 800 km, firstly at an inclination of 80° (where we find the peak in the map in Figure 6) and then at 100°. Before investigating the evolution of the capacity associated with these scenarios, it is interesting to look at the evolution of the number of objects along the simulation. This is depicted in Figure 7, where it is possible to appreciate how, after an initial difference, the trends tend to converge toward the reference scenario. This can be explained by the fact that at this altitude some of the fragments will re-enter, and, additionally, the DELTA4 model will add new fragmentation every years and thus will increase the number of objects.

Looking at the evolution of the space capacity over time, Figure 8 shows how at first the value is greater in both cases, and then converges to the reference. This implies that, after an initial period, the level of consumed capacity returns to that of the reference scenario.

The same thing can be appreciated investigating the difference between the scenarios with fragmentation and the reference scenario by applying the model introduced in Section 3.2.

Both the scenarios fall into the level of risk “high”, but the case at higher inclination (in red) tends faster toward the baseline with respect to the case at lower inclination (in dark blue). This can be explained by the fact that fragmentation at 80° puts fragments in a geometrically more dangerous position for most of the satellites, namely those in sun synchronous orbit (about 100°), in

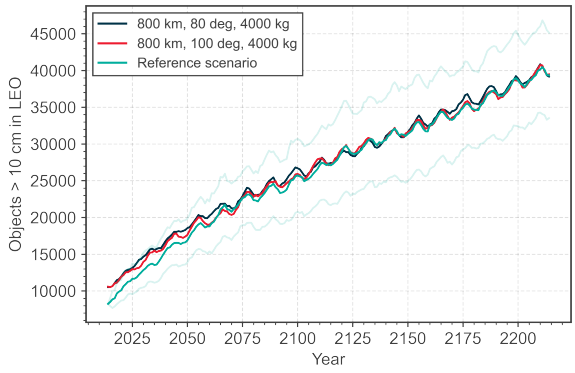

Fig. 7. Evolution of the number of objects larger than 10 cm over time considering two fragmentation at the same altitude but different inclination - LEO.

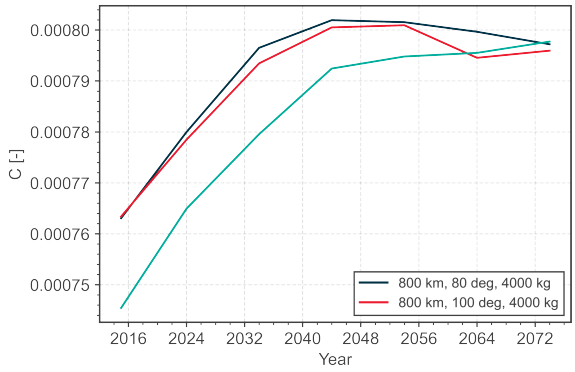

Fig. 8. Capacity evolution over time (mean value for all the MC) - same altitude, different inclination.

terms of collision probability and severity. Indeed, this is a result that could also be inferred by looking at the effects map (Figure 6), where the peak in terms of severity of a fragmentation is at 800 km altitude and 80° in inclination.

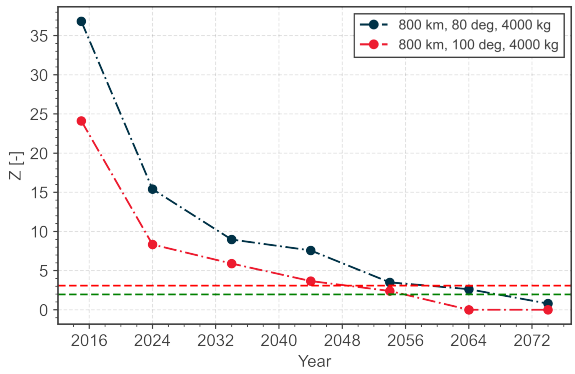

Fig. 9. Z-score evolution over time - same altitude, different inclination.

A third fragmentation involving a mass of 8000 kg was simulated at an altitude of 1600 km and an inclination of 80°, and the evolution of the number of ob-

jects larger than 10 cm is show in Figure 10. If the fragmentation occurs at a higher altitude, the fragments take longer to re-enter, and this may explain why the trend remains above than the reference scenario.

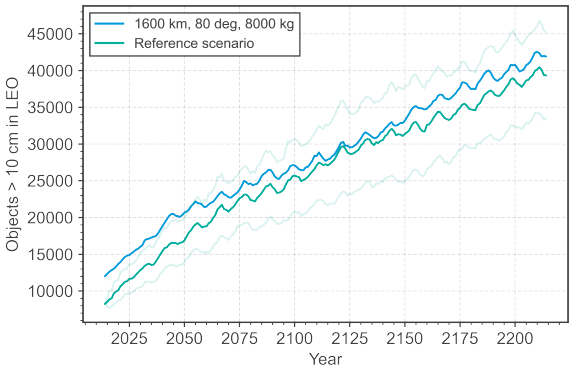

Fig. 10. Evolution of the number of objects larger than 10 cm over time considering a fragmentation at high altitude - LEO.

Figure 11 shows how, in this third case, the risk level of the fragmentation is "low". This is related to the fact that fragmentation introduces fragments that do not go into high risk regions for orbiting satellites, thus not going to affect the probability of collision.

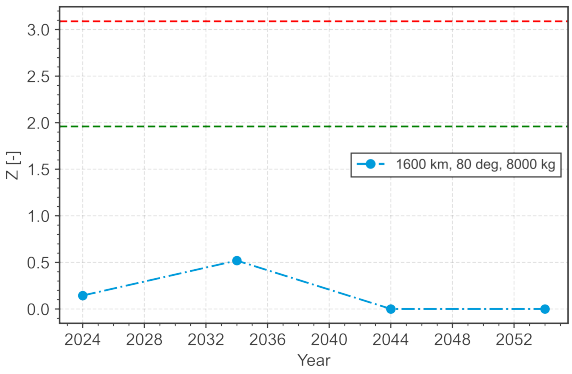

Fig. 11. Z-score evolution over time - higher altitude.

4.3 Space capacity Z-score evolution for fragmentation with different masses

In the second case, the position of the fragment is considered fixed (i.e., altitude at 800 km and inclination at 80°) and the mass involved is changed. The results are shown in Figure 12, where it can be seen that as the mass decreases the trend tends faster toward that of the reference scenario. This is probably due to the fact that fragmentation is hidden because of the other fragmentations simulated by the evolutionary model.

Figure 13 shows, instead, the evolution over time of the space capacity for each simulated scenario. The

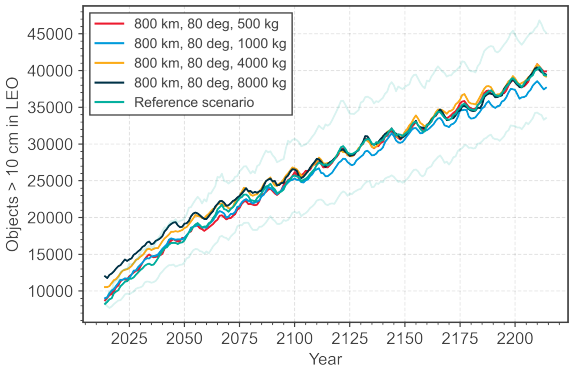

Fig. 12. Evolution of the number of objects larger than 10 cm over time considering different masses involved in the fragmentation - LEO.

common feature concerns the beginning increase in capacity, and then having a decrease that tends to the capacity value of the reference scenario. Indeed, the reference scenario is the only one characterised by a constant increase.
This behavior can be explained by looking at what also happens to the number of objects, that is, an initial higher level and then trending toward a similar value. This results in similarity in the background population and thus in an alignment of the probability of collision in the various scenarios.

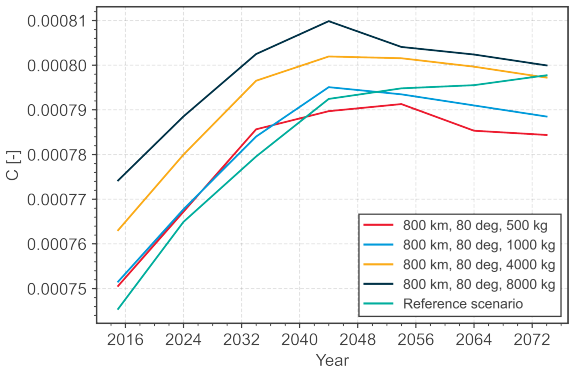

Fig. 13. Capacity evolution over time (mean value for alle the MC) - different masses.

Figure 14 shows the Z-score evolution over time of the four cases of the fragmentation with the fixed location and the change in the mass. As expected, by decreasing the mass the level of risk decreases (still remaining high) and it is reabsorbed faster by the space environment.

5. Conclusion and future works

The sustainability of the space around the Earth is becoming an increasingly important issue in the space sector. This because many new objects are launched and many fragmentation events occur each year. The latter

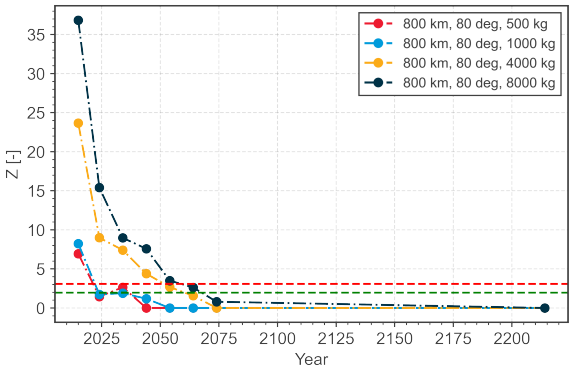

Fig. 14. Z-score evolution over time - different masses.

are monitored, reconstructed, and studied to investigate the risk of collision with the population of active satellites. However, understand the level of risk posed by a new fragmentation event over short- and long- period of time is also important.

The aim of this work was to investigate the possibility of using capacity models of the space environment to assign a the level of risk caused by a fragmentation. This is done by comparing the evolution of a reference scenario (defined in terms of initial population, launch traffic, and PMD strategy) with the same one but with the addition of a fragmentation using the one-tailed Z test.

The proposed model showed how it is possible to combine the space capacity metric and the investigation of fragmentation. Indeed, the results showed that this tool provides a different perspective than simply computing the number of objects and studying the long-term evolution.

The work is still in progress and involves further study in comparing the evolution of the number of objects, of possible chain effects due to the generated fragments (having available information on the additional fragmentations generated), other orbit geometry. In addition, the model could be applied to real scenarios (e.g., a fragmentation that actually occurred) by reproducing the populations and the event.

Acknowledgements

This work was funded by the European Research Council (ERC) under the European Union's Horizon 2020 research and innovation programme (grant agreement No 101089265 - GREEN SPECIES).

Appendix A (Fragmentation severity map)

The computation of the severity term is carried out using the STARLING 2.1 tool, and two steps are needed: the selection of targets representative of the population of active objects, and the evaluation of the cumulative collision probability of dummy fragmentation with the reference targets selected. All the steps are performed considering a grid in Keplerian orbital elements, specifically in semi-major axis and inclination for the LEO objects.

In the grid, a target is defined in each bin where the cumulative cross-sectional area of all the objects in the bin exceeds a defined threshold (25 km for this work). The target will have the average physical properties of all objects included in the bin.

The effect of each fragmentation event, carried out on the same grid, is evaluated according to the following three steps:

- Estimation of the initial fragments density distribution, through a probabilistic reformulation of the NASA Standard Breakup Model (SBM) [26] [21].
- Propagation of the fragments density through the Method Of Characteristics (MOC) [27], and consequent characteristics' interpolation through binning in the 7D phase space of Keplerian elements and area-to-mass ratio [21].
- Evaluation of the cumulative number of impacts against each representative target over the considered time frame [20]. The representative targets cross-sectional area is here assumed to be unitary (the result is re-scaled a posteriori).

The procedure gives as output maps similar to the one presented in the Figure 15.

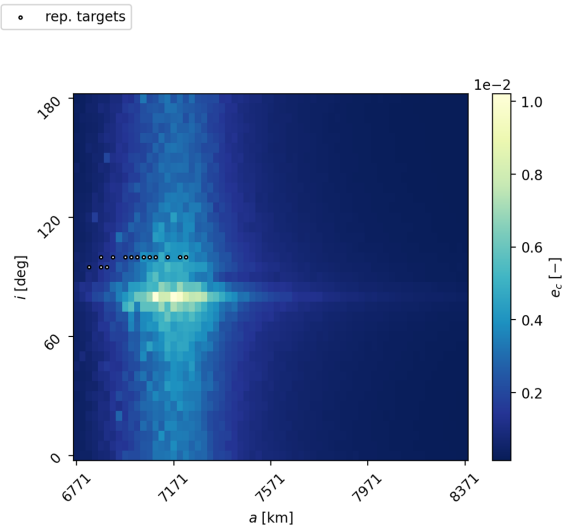

Fig. 15. Catastrophic collision effect maps computed considering targets at 01-01-2014.

Appendix B (Capacity samples from normal distribution)

Due to computing resources, only 40 MC simulations were calculated for each test case. Since the Z-test 3 re-

quires a normal distribution in order to work, capacity samples were checked.
The test was performed considering the Shapiro-Wilk test [28], typically used to test the null hypothesis that the data was drawn from a normal distribution. The test result is the p-value for the hypothesis test which, for samples taken from a normal distribution, gives a result greater than 0.05.
Table 2 summarises some of the results of the test for the different capacity distributions.
However, it is important to mention that, in general, evolution model are not normal [29]. This was the first attempt to address the problem, and further investigations will be conducted in the future.

References

[1] ESA Space Debris Office, "Esa's annual space environment report," Tech. rep., Technical report, 2024, `https://www.sdo.esoc.esa.int/environment_report/Space_Environment_Report_latest.pdf`.

[2] McKnight, D., Witner, R., Letizia, F., Lemmens, S., Anselmo, L., Pardini, C., Rossi, A., Kunstadter, C., Kawamoto, S., Aslanov, V., Dolado Perez, J.-C., Ruch, V., Lewis, H., Nicolls, M., Jing, L., Dan, S., Dongfang, W., Baranov, A., and Grishko, D., "Identifying the 50 statistically-most-concerning derelict objects in LEO," *Acta Astronautica*, Vol. 181, 2021, pp. 282–291.

[3] Letizia, F., Colombo, C., Rossi, A., Muciaccia, A., Giudici, L., Harada, R., Kawamoto, S., and Böttcher, L., "Mission-based and environment-based approaches for assessing the severity of a space debris evolution scenario from a sustainability perspective," *75th International Astronautical Congress (IAC), Milan, Italy*, 10 2024.

[4] Letizia, F., Bastida Virgili, B., and Lemmens, S., "Assessment of orbital capacity thresholds through long-term simulations of the debris environment," *Advances in Space Research*, Vol. 72, No. 7, 2023, pp. 2552–2569.

[5] D'Ambrosio, A. and Linares, R., "Carrying Capacity of Low Earth Orbit Computed using Source-Sink Models," *Journal of Spacecraft and Rockets*, 04 2024.

[6] Bastida Virgili, B., "DELTA (DEBRIS ENVIRONMENT LONG-TERM ANALYSIS)," *6th International Conference on Astrodynamics Tools and Techniques (ICATT), Darmstadt, Germany*, 03 2016.

[7] Liou, J.-C., Hall, D., Krisko, P., and Opiela, J., "LEGEND – a three-dimensional LEO-to-GEO debris evolutionary model," *Advances in Space Research*, Vol. 34, No. 5, 2004, pp. 981–986, Space Debris.

[8] Jc, D.-P., Romain, D., and Bruno, R., "Introducing MEDEE–A new orbital debris evolutionary model," *Proceeding of the 6th European Conference on Space Debris*, 2013.

[9] Rossi, A., Anselmo, L., Pardini, C., Jehn, R., and Valsecchi, G., "The new space debris mitigation (SDM 4.0) long term evolution code," *5th European Conference on Space Debris, Darmstadt, Germany*, Vol. 672, 01 2009.

[10] Rossi, A., Anselmo, L., Cordelli, A., Farinella, P., and Pardini, C., "Modelling the evolution of the space debris population," *Planetary and Space Science*, Vol. 46, No. 11, 1998, pp. 1583–1596, Second Italian Meeting on Celestial Mechanics.

[11] Somma, G. L., *Adaptive remediation of the space debris environment using feedback control*, Ph.D. thesis, University of Southampton, July 2019.

[12] D'Ambrosio, A., Servadio, S., Mun Siew, P., and Linares, R., "Novel Source–Sink Model for Space Environment Evolution with Orbit Capacity Assessment," *Journal of Spacecraft and Rockets*, Vol. 60, No. 4, 2023, pp. 1112–1126.

[13] Letizia, F., Colombo, C., Lewis, H., and Krag, H., "Development of a debris index," *Stardust Final Conference - Advances in Asteroids and Space Debris Engineering and Science*, Vol. 52, Springer, February 2018, pp. 191–206.

[14] Colombo, C., Trisolini, M., Muciaccia, A., Giudici, L., Gonzalo, Juan Luis; Frey, S., Del Campo, B., Letizia, F., and Lemmens, S., "Evaluation of the space capacity share used by a mission," *73nd International Astronautical Congress, Paris, France*, 2022.

[15] Colombo, C., Giudici, L., Muciaccia, A., Gonzalo, J. L., Borja, D. C., Vyavahare, N., Dutra, D., Letizia, F., and Lemmens, S., "Assessment of the collision risk in orbital slots and the overall space capacity," *2nd International Orbital Debris Conference, Sugar Land, Texas*, 12 2023.

[16] Letizia, F., Colombo, C., Lewis, H. G., and Krag, H., "Assessment of breakup severity on operational satellites," *Advances in Space Research*, Vol. 58, No. 7, 2016, pp. 1255–1274.

[17] Muciaccia, A., Trisolini, M., Giudici, L., Gonzalo, J. L., Colombo, C., and Letizia, F., "Influence of Constellations on Current and Future Missions," *2nd International Orbital Debris Conference, Sugar Land, Texas*, 12 2023.

Table 2. P-value as results of the Shapiro-Wilk test for the different capacity distribution of the different fragmentation events.

Scenario	2015	2024	2034	2044	2054	2064	2074
Reference scenario	0.137	0.880	0.151	0.348	0.674	0.736	0.583
800 km, 80 deg, 8000 kg	0.091	0.530	0.248	0.836	0.496	0.007	0.884

[18] Muciaccia, A., Giudici, L., Trisolini, M., Colombo, C., Borja, D. C., Letizia, F., and Lemmens, S., "Space environment investigation using a space debris index," *9th Space Traffic Management Conference, Austin, Texas*, 2 2023.

[19] Giudici, L., Gonzalo, J. L., Muciaccia, A., Colombo, C., Trisolini, M., and Letizia, F., "Environmental impact of object breakup in medium-Earth orbit," *Advances in Space Research*, Vol. 74, No. 4, 2024, pp. 1900–1915.

[20] Giudici, L., Gonzalo, J. L., and Colombo, C., "Density-based in-orbit collision risk model valid for any impact geometry," *Acta Astronautica*, Vol. 219, 2024, pp. 785–803.

[21] Giudici, L., Trisolini, M., and Colombo, C., "Probabilistic multi-dimensional debris cloud propagation subject to non-linear dynamics," *Advances in Space Research*, Vol. 72, No. 2, 2023, pp. 129–151.

[22] Kessler, D. J. and Cour-Palais, B. G., "Collision frequency of artificial satellites: The creation of a debris belt," *Journal of Geophysical Research: Space Physics*, Vol. 83, No. A6, 1978, pp. 2637–2646.

[23] Johnson, N., Krisko, P., Liou, J.-C., and Anz-Meador, P., "NASA's new breakup model of evolve 4.0," *Advances in Space Research*, Vol. 28, No. 9, 2001, pp. 1377–1384.

[24] Rossi, A., Lewis, H., White, A., Anselmo, L., Pardini, C., Krag, H., and Bastida Virgili, B., "Analysis of the consequences of fragmentations in low and geostationary orbits," *Advances in Space Research*, Vol. 57, No. 8, 2016, pp. 1652–1663.

[25] Rossi, A., Lewis, H., Alessi, E. M., Valsecchi, G. B., White, A., Anselmo, L., and Pardini, C., "Fragmentation Consequence Analysis for LEO and GEO Orbits, Version 1.0. Executive Summary, ESA/ESOC No," Tech. rep., 4000106534/12/F/MOS, July, 2015.

[26] Frey, S. and Colombo, C., "Transformation of Satellite Breakup Distribution for Probabilistic Orbital Collision Hazard Analysis," *Journal of Guidance, Control, and Dynamics*, Vol. 44, No. 1, 2021, pp. 88–105.

[27] Johnson, N. L., LaSalle, J. P., and Sirovich, L., *Partial Differential Equations*, Springer, 1981.

[28] SHAPIRO, S. S. and WILK, M. B., "An analysis of variance test for normality (complete samples)†," *Biometrika*, Vol. 52, No. 3-4, 12 1965, pp. 591–611.

[29] Lidtke, A. A., Lewis, H. G., and Armellin, R., "Statistical analysis of the inherent variability in the results of evolutionary debris models," *Advances in Space Research*, Vol. 59, No. 7, 2017, pp. 1698–1714.